Casimir pressure in peptide films on metallic substrates: Change of sign via graphene coating

G. L. Klimchitskaya,[1,2] V. M. Mostepanenko [ORCID],[1,2,3] and E. N. Velichko [ORCID][2]

[1]*Central Astronomical Observatory at Pulkovo of the Russian Academy of Sciences, Saint Petersburg 196140, Russia*

[2]*Institute of Physics, Nanotechnology and Telecommunications, Peter the Great Saint Petersburg Polytechnic University, Saint Petersburg 195251, Russia*

[3]*Kazan Federal University, Kazan 420008, Russia*

We find that the Casimir pressure in peptide films deposited on metallic substrates is always repulsive which makes these films less stable. It is shown that by adding a graphene sheet on top of peptide film one can change the sign of the Casimir pressure by making it attractive. For this purpose, the formalism of the Lifshitz theory is extended to the case when the film and substrate materials are described by the frequency-dependent dielectric permittivities, whereas the response of graphene to the electromagnetic field is governed by the polarization tensor in (2+1)-dimensional space-time found in the framework of the Dirac model. Both pristine and gapped and doped graphene sheets are considered possessing some nonzero energy gap and chemical potential. According to our results, in all cases the presence of graphene sheet makes the Casimir pressure in peptide film deposited on a metallic substrate attractive starting from some minimum film thickness. The value of this minimum thickness becomes smaller with increasing chemical potential and larger with increasing energy gap and the fraction of water in peptide film. The physical explanation for these results is provided, and their possible applications in organic electronics are discussed.

I. INTRODUCTION

Considerable recent attention has been focused on organic materials which combine electrical conductivity with high mechanical flexibility. Carbon-based materials of this type have gained widespread acceptance in organic electronics [1] giving rise to creation of innovative electronic devices, such as solar cells [2,3], field-effect transistors [4–7], light-emitting diodes [8,9], biomarkers [10–12], etc. Many of the organic electronic devices employ thin peptide films deposited on dielectric and metallic substrates for their functionality [13–19]. Physical phenomena at organic-dielectric and organic-metal interfaces have been the subject of much investigation (see, e.g., Refs. [20–30]).

One of these phenomena, which becomes essential in films of less than 1 μm thickness, is caused by the zero-point and thermal fluctuations of the electromagnetic field. Fluctuations result in the van der Waals and Casimir forces between two closely spaced material layers separated by a vacuum gap [31,32] as well as in the internal free energies and pressures induced in both freestanding and deposited on a substrate film. The van der Waals and Casimir free energies and forces in layer structures can be expressed via the frequency-dependent dielectric permittivities of interacting layers by means of the Lifshitz theory [33]. In Refs. [34–37], this theory was applied for calculation of the van der Waals forces between films made of organic materials. Based on the Lifshitz theory, the Casimir free energy and pressure were also investigated for the freestanding and deposited on substrate metallic and dielectric films [38–43].

The fluctuation-induced free energy of both freestanding and deposited on dielectric and metallic substrate peptide films was found in Ref. [44]. For this purpose, a representation for the dielectric permittivity of a typical model peptide along the imaginary frequency axis was suggested using the results of Ref. [45] for electrically neutral 18-residue zinc finger peptide in the microwave region and of Ref. [46] for cyclic tripeptide RGD-4C in the ultraviolet region. The behavior of the dielectric permittivity of typical peptide in the region of infrared frequencies was modeled in the Ninham-Parsegian representation.

It was shown that the fluctuation-induced free energy of peptide films deposited on metallic substrates is positive, whereas for dielectric substrates it can change its sign depending on the film thickness [44]. The effect of sign change arising in the case of dielectric substrates was considered in more detail in Refs. [47,48]. According to the obtained results, for sufficiently thick peptide films (thicker than 135 nm for a film containing 10% of water deposited on a SiO$_2$ substrate) the fluctuation-induced Casimir pressure becomes negative. This corresponds to attraction of a film to a substrate and makes film more stable. In Ref. [49] it was shown that the doping of peptide film deposited on a dielectric substrate with metallic nanoparticles results in a wider range of film thicknesses, where the Casimir pressure is attractive, and further increases the film stability.

In this paper, we consider peptide films deposited on metallic substrates and show that the fluctuation-induced pressure is positive which corresponds to a repulsive force and makes the peptide film less stable. The doping of peptide with metallic nanoparticles is not helpful in this case because it does not change the sign of the Casimir pressure in films deposited on metallic substrates. In order to make peptide films on

245421-1

metallic substrates more stable, we propose to coat an additional graphene sheet on top of peptide film.

The fluctuation-induced Casimir pressure in a material layer sandwiched between a sufficiently thick metallic plate and a graphene sheet has not been investigated so far. This is a familiar three-layer system where, however, one layer is two-dimensional. Because of this, the Lifshitz formula for the Casimir pressure should contain the standard reflection coefficients on the boundary surface between peptide and metal (which are expressed via the respective dielectric permittivities) and more sophisticated ones on the boundary between peptide and graphene (which also depend on the polarization tensor of graphene [50]). Here, we present the necessary formalism describing this system based on the first principles of quantum electrodynamics at nonzero temperature.

Using the developed formalism, we have calculated the Casimir pressure in pure peptide films and in peptide films containing different fractions of water sandwiched between an Au substrate and a graphene sheet with various values of the energy gap or chemical potential. It is shown that the coating by a pristine graphene sheet on top of pure peptide film makes the Casimir pressure in this film negative for film thicknesses exceeding 211.7 nm. In so doing, for graphene with a nonzero chemical potential the Casimir pressure becomes attractive starting from smaller film thicknesses whereas for graphene with a nonzero energy gap the same goal is reached for thicker films.

Special attention is devoted to the most realistic case when a peptide film contains some fraction of water and a graphene sheet is characterized by the nonzero energy gap and chemical potential. It is shown that in all cases the Casimir pressure in peptide film becomes attractive for film thicknesses exceeding some definite value wherein the pressure vanishes. This value depends on the fraction of water in the film and on the values of the energy gap and chemical potential of a graphene sheet. It is smaller for peptide films with a smaller fraction of water, larger chemical potential, and smaller energy gap of graphene. By contrast, for a larger fraction of water, smaller chemical potential, and larger energy gap of graphene the value of film thickness, such that the Casimir pressure takes zero value, increases.

The obtained results could be useful for prospective devices of organic electronics with further reduced dimensions to ensure their stability.

The paper is organized as follows. In Sec. II, the general formalism is presented allowing calculation of the Casimir pressure in thin film sandwiched between a metallic plate and a graphene sheet. Section III is devoted to an impact of graphene coating on the Casimir pressure in pure (dried) peptide film. The most realistic case of peptide films containing some fraction of water and graphene films possessing the nonzero energy gap and chemical potential is considered in Sec. IV. Section V presents our conclusions and a discussion.

II. FORMALISM FOR THE CASIMIR PRESSURE IN A FILM SANDWICHED BETWEEN METALLIC PLATE AND GRAPHENE SHEET

We consider the Casimir pressure in a peptide film of thickness a characterized by the frequency-dependent dielectric

permittivity $\varepsilon^{(1)}(\omega)$ deposited on metallic substrate with the dielectric permittivity $\varepsilon^{(2)}(\omega)$. The sheet of graphene possessing the energy gap Δ and chemical potential μ is coated on the top of peptide film. This system is kept at temperature T in thermal equilibrium with the environment.

For the purpose of numerical computations, it is convenient to use the dimensionless variables,

$$\zeta_l = \frac{2a\xi_l}{c}, \quad y = 2a\left(k_\perp^2 + \frac{\xi_l^2}{c^2}\right)^{1/2}, \quad (1)$$

where $\xi_l = 2\pi k_B T l/\hbar$ are the Matsubara frequencies, k_B is the Boltzmann constant, and $k_\perp$ is the projection of the wave vector on the plane of a film (which is perpendicular to the Casimir force).

Then, the Casimir pressure in a peptide film is given by the Lifshitz formula [31–33],

$$P(a, T) = -\frac{k_B T}{8\pi a^3} \sum_{l=0}^{\infty}{}' \int_{\zeta_l}^{\infty} y k^{(1)}(\zeta_l, y) dy$$

$$\times \sum_{\kappa} \frac{1}{\left[R_\kappa(\zeta_l, y) r_\kappa^{(1.2)}(\zeta_l, y)\right]^{-1} e^{k^{(1)}(\zeta_l, y)} - 1}, \quad (2)$$

where

$$k^{(n)}(\zeta_l, y) = \left[y^2 + \left(\varepsilon_l^{(n)} - 1\right)\zeta_l^2\right]^{1/2}, \quad (3)$$

$\varepsilon_l^{(n)} = \varepsilon^{(n)}(i\xi_l) = \varepsilon^{(n)}[ic\zeta_l/(2a)], n = 1, 2$ for a peptide and a substrate metal, respectively, a prime on the summation sign divides the term with $l = 0$ by 2, and the sum in κ is over two polarizations of the electromagnetic field—transverse magnetic ($\kappa = $ TM) and transverse electric ($\kappa = $ TE).

The quantities $r_\kappa^{(1,2)}$ and R_κ in Eq. (2) are the reflection coefficients on the boundary planes between the peptide film and metallic substrate and between the peptide film and graphene sheet, respectively. Note that the metallic substrate is considered as a semispace (for this purpose its thickness should be larger than 100 nm [32]).

An explicit form of the coefficients $r_\kappa^{(1,2)}$ is well known. These are the familiar Fresnel reflection coefficients calculated at the pure imaginary Matsubara frequencies,

$$r_{\text{TM}}^{(1,2)}(\zeta_l, y) = \frac{\varepsilon_l^{(2)} k^{(1)}(\zeta_l, y) - \varepsilon_l^{(1)} k^{(2)}(\zeta_l, y)}{\varepsilon_l^{(2)} k^{(1)}(\zeta_l, y) + \varepsilon_l^{(1)} k^{(2)}(\zeta_l, y)},$$

$$r_{\text{TE}}^{(1,2)}(\zeta_l, y) = \frac{k^{(1)}(\zeta_l, y) - k^{(2)}(\zeta_l, y)}{k^{(1)}(\zeta_l, y) + k^{(2)}(\zeta_l, y)}. \quad (4)$$

The reflection coefficients R_κ on the boundary plane between peptide and graphene are more involved. If a peptide film and a graphene sheet are separated by a vacuum gap of width d, the reflection coefficient takes the form [32],

$$R_\kappa(\zeta_l, y; d) = \frac{r_\kappa^{(1,0)}(\zeta_l, y) + r_\kappa^{(\text{gr})}(\zeta_l, y) e^{-dy/a}}{1 + r_\kappa^{(1,0)}(\zeta_l, y) r_\kappa^{(\text{gr})}(\zeta_l, y) e^{-dy/a}}. \quad (5)$$

Here, $r_\kappa^{(1,0)}$ are the Fresnel reflection coefficients on the boundary between a peptide semispace and vacuum which are expressed via the dielectric permittivity of

peptide $\varepsilon_l^{(1)}$ as

$$r_{\mathrm{TM}}^{(1,0)}(\zeta_l, y) = \frac{k^{(1)}(\zeta_l, y) - \varepsilon_l^{(1)} y}{k^{(1)}(\zeta_l, y) + \varepsilon_l^{(1)} y},$$

$$r_{\mathrm{TE}}^{(1,0)}(\zeta_l, y) = \frac{k^{(1)}(\zeta_l, y) - y}{k^{(1)}(\zeta_l, y) + y}. \qquad (6)$$

The reflection coefficients $r_\kappa^{(\mathrm{gr})}$ in Eq. (5) are on a freestanding in a vacuum graphene sheet. These are the non-Fresnel coefficients whose exact form is expressed in the framework of the Dirac model [51] via the polarization tensor of graphene in (2+1)-dimensional space-time,

$$\Pi_{mn}(i\xi_l, k_\perp, T, \Delta, \mu) \equiv \Pi_{mn,l}(k_\perp, T, \Delta, \mu), \qquad (7)$$

or, in the dimensionless form,

$$\tilde{\Pi}_{mn,l}(y, T, \Delta, \mu) = \frac{2a}{\hbar} \Pi_{mn,l}(k_\perp, T, \Delta, \mu), \qquad (8)$$

where m, $n = 0, 1, 2$.

The explicit expressions for the coefficients $r_\kappa^{(\mathrm{gr})}$ are the following (see Refs. [52,53] and also Refs. [54,55] where the dimensionless quantities are used):

$$r_{\mathrm{TM}}^{(\mathrm{gr})}(\zeta_l, y) = \frac{y\tilde{\Pi}_{00,l}(y, T, \Delta, \mu)}{y\tilde{\Pi}_{00,l}(y, T, \Delta, \mu) + 2(y^2 - \zeta_l^2)},$$

$$r_{\mathrm{TE}}^{(\mathrm{gr})}(\zeta_l, y) = -\frac{\tilde{\Pi}_l(y, T, \Delta, \mu)}{\tilde{\Pi}_l(y, T, \Delta, \mu) + 2y(y^2 - \zeta_l^2)}, \qquad (9)$$

where the quantity

$$\tilde{\Pi}_l(y, T, \Delta, \mu) \equiv (y^2 - \zeta_l^2)\mathrm{tr}\tilde{\Pi}_{mn,l}(y, T, \Delta, \mu) - y^2 \tilde{\Pi}_{00,l}(y, T, \Delta, \mu) \qquad (10)$$

is expressed via the tensor trace $\mathrm{tr}\tilde{\Pi}_{mn,l} \equiv \tilde{\Pi}_{m,l}^m$.

Before presenting the exact expressions for the components of the polarization tensor, we conclude that the reflection coefficients R_κ entering Eq. (2) are obtained from Eq. (5) in the limiting case $d \to 0$:

$$R_\kappa(\zeta_l, y) = \lim_{d \to 0} R_\kappa(\zeta_l, y; d)$$

$$= \frac{r_\kappa^{(1,0)}(\zeta_l, y) + r_\kappa^{(\mathrm{gr})}(\zeta_l, y)}{1 + r_\kappa^{(1,0)}(\zeta_l, y) r_\kappa^{(\mathrm{gr})}(\zeta_l, y)}, \qquad (11)$$

where $r_\kappa^{(1,0)}$ and $r_\kappa^{(\mathrm{gr})}$ are defined in Eqs. (6) and (9), respectively.

It only remains to present the expressions for $\tilde{\Pi}_{00,l}$ and $\tilde{\Pi}_l$. We write out these expressions in the form allowing immediate analytic continuation over the entire plane of complex frequencies [56,57] and use the dimensionless quantities [54,55].

We start with the case $l = 0$. In this case the exact expressions for $\tilde{\Pi}_{00,0}$ and $\tilde{\Pi}_0$ are given by [54,55]

$$\tilde{\Pi}_{00,0}(y, T, \Delta, \mu) = \frac{\alpha y}{\tilde{v}_F}\Psi(D_0) + \frac{16\alpha}{\tilde{v}_F^2}\frac{ak_BT}{\hbar c}\ln[(e^{\frac{\mu}{k_BT}} + e^{-\frac{\Delta}{2k_BT}})(e^{-\frac{\mu}{k_BT}} + e^{-\frac{\Delta}{2k_BT}})]$$

$$- \frac{4\alpha y}{\tilde{v}_F}\int_{D_0}^{\sqrt{1+D_0^2}} du\, w_0(u, y, T, \mu)\frac{1 - u^2}{(1 - u^2 + D_0^2)^{1/2}},$$

$$\tilde{\Pi}_0(y, T, \Delta, \mu) = \alpha\tilde{v}_F y^3\Psi(D_0) + 4\alpha\tilde{v}_F y^3\int_{D_0}^{\sqrt{1+D_0^2}} du\, w_0(u, y, T, \mu)\frac{-u^2 + D_0^2}{(1 - u^2 + D_0^2)^{1/2}}. \qquad (12)$$

Here, the following notations are introduced:

$$\Psi(x) = 2[x + (1 - x^2)\arctan x^{-1}],$$

$$w_l(u, y, T, \mu) = \frac{1}{e^{B_l u + \frac{\mu}{k_BT}} + 1} + \frac{1}{e^{B_l u - \frac{\mu}{k_BT}} + 1},$$

$$B_l = B_l(y, T) = \frac{\hbar c}{4ak_BT}p_l(y),$$

$$D_l = D_l(y) = \frac{2a\Delta}{\hbar c\, p_l(y)},$$

$$p_l(y) = [\tilde{v}_F^2 y^2 + (1 - \tilde{v}_F^2)\zeta_l^2]^{1/2}, \qquad (13)$$

and $\tilde{v}_F = v_F/c \approx 1/300$, $\alpha = e^2/(\hbar c) \approx 1/137$ are the dimensionless Fermi velocity for graphene and the fine structure constant, respectively.

Now we consider the expressions for $\tilde{\Pi}_{00,l}$ and $\tilde{\Pi}_l$ with $l \geqslant 1$. In this case it is unnecessary to use rather cumbersome exact formulas because at $T = 300$ K and film thicknesses $a > 50$ nm it holds $\zeta_l \gg \tilde{v}_F$ for all $l \geqslant 1$. As a result

[54,55,58],

$$\tilde{\Pi}_{00,l}(y, T, \Delta, \mu) \approx \frac{\alpha(y^2 - \zeta_l^2)}{\zeta_l}[\Psi(\Delta_l) + \tilde{Y}_l(y, T, \Delta, \mu)],$$

$$\tilde{\Pi}_l(y, T, \Delta, \mu) \approx \alpha\zeta_l(y^2 - \zeta_l^2)[\Psi(\Delta_l) + \tilde{Y}_l(y, T, \Delta, \mu)], \qquad (14)$$

where $\Delta_l = 2a\Delta/(\hbar c\zeta_l)$ and the quantity $\tilde{Y}_l$ is defined as

$$\tilde{Y}_l(y, T, \Delta, \mu)$$

$$= 2\int_{\Delta_l}^{\infty} du\, w_l(u, y, T, \mu)\frac{u^2 + \Delta_l^2}{u^2 + 1}$$

$$\approx 2\int_{\Delta_l}^{\infty} du\left(\frac{1}{e^{\pi l u + \frac{\mu}{k_BT}} + 1} + \frac{1}{e^{\pi l u - \frac{\mu}{k_BT}} + 1}\right)\frac{u^2 + \Delta_l^2}{u^2 + 1}. \qquad (15)$$

In the last equation, we have taken into account that the major contribution to Eq. (2) is given by $y \sim 1$. Computations

show [58] that Eqs. (14) and (15) lead to less than 0.02% relative error in the obtained Casimir pressures.

The reflection coefficients (9) on a graphene sheet with $l = 0$ are simplified to

$$r_{\text{TM}}^{(\text{gr})}(0, y) = \frac{\tilde{\Pi}_{00,0}(y, T, \Delta, \mu)}{\tilde{\Pi}_{00,0}(y, T, \Delta, \mu) + 2y},$$

$$r_{\text{TE}}^{(\text{gr})}(0, y) = -\frac{\tilde{\Pi}_0(y, T, \Delta, \mu)}{\tilde{\Pi}_0(y, T, \Delta, \mu) + 2y^3}, \quad (16)$$

where $\tilde{\Pi}_{00,0}$ and $\tilde{\Pi}_0$ are defined in Eq. (12).

By putting $l = 0$ in Eq. (6), one obtains

$$r_{\text{TM}}^{(1,0)}(0, y) = \frac{1 - \varepsilon_0^{(1)}}{1 + \varepsilon_0^{(1)}}, \quad r_{\text{TE}}^{(1,0)}(0, y) = 0. \quad (17)$$

Substituting Eqs. (16) and (17) in Eq. (11), we arrive at

$$R_{\text{TM}}(0, y) = \frac{\tilde{\Pi}_{00,0}(y, T, \Delta, \mu) + y(1 - \varepsilon_0^{(1)})}{\tilde{\Pi}_{00,0}(y, T, \Delta, \mu) + y(1 + \varepsilon_0^{(1)})},$$

$$R_{\text{TE}}(0, y) = r_{\text{TE}}^{(\text{gr})}(0, y). \quad (18)$$

For all $l \geqslant 1$ the reflection coefficients (11) are obtained with the help of Eqs. (6), (9), and (14),

$$R_{\text{TM}}(\zeta_l, y) = \frac{k^{(1)}(\zeta_l, y)\{\alpha[\Psi(\Delta_l) + \tilde{Y}_l]y + \zeta_l\} - \varepsilon_l^{(1)}\zeta_l y}{k^{(1)}(\zeta_l, y)\{\alpha[\Psi(\Delta_l) + \tilde{Y}_l]y + \zeta_l\} + \varepsilon_l^{(1)}\zeta_l y},$$

$$R_{\text{TE}}(\zeta_l, y) = \frac{k^{(1)}(\zeta_l, y) - y - \alpha[\Psi(\Delta_l) + \tilde{Y}_l]\zeta_l}{k^{(1)}(\zeta_l, y) + y + \alpha[\Psi(\Delta_l) + \tilde{Y}_l]\zeta_l}, \quad (19)$$

where $\Psi(\Delta_l)$ and $\tilde{Y}_l$ are defined in Eqs. (13) and (15).

Now that we have presented the required formalism, the Casimir pressure in a peptide film can be computed by Eq. (2) using the reflection coefficients (4), (18), and (19). Calculations of this kind are performed in the next sections for different parameters of a peptide film and a graphene sheet.

III. IMPACT OF GRAPHENE COATING ON THE CASIMIR PRESSURE IN DRIED PEPTIDE FILMS

In this section, we consider a somewhat idealized situation when the film is made of pure dried peptide, which does not contain water, and graphene is pristine or is characterized either by some nonzero chemical potential μ or by a nonzero energy gap Δ.

In the absence of graphene, the Casimir free energy of peptide films (both dried and containing some fraction Φ of water) deposited on an Au substrate was found in Ref. [44]. For this purpose, by combining available information about the optical properties of two closely similar peptides in different frequency regions (see Sec. I), the values of dielectric permittivities of typical peptides $\varepsilon_l^{(1)}$ containing the fractions of water $\Phi = 0$, 0.1, 0.25, and 0.4 were found at the pure imaginary Matsubara frequencies $i\xi_0 = 0$, $i\xi_1$, $i\xi_2$, ..., $i\xi_{30}$ (see Fig. 2 of Ref. [44]). These values are used in all computations below. It was shown [44] that the Casimir free energy of peptide films with any Φ on an Au substrate is positive and decreases with increasing film thickness.

We begin with similar computations for the Casimir pressure performed by using Eq. (2) where in the absence of
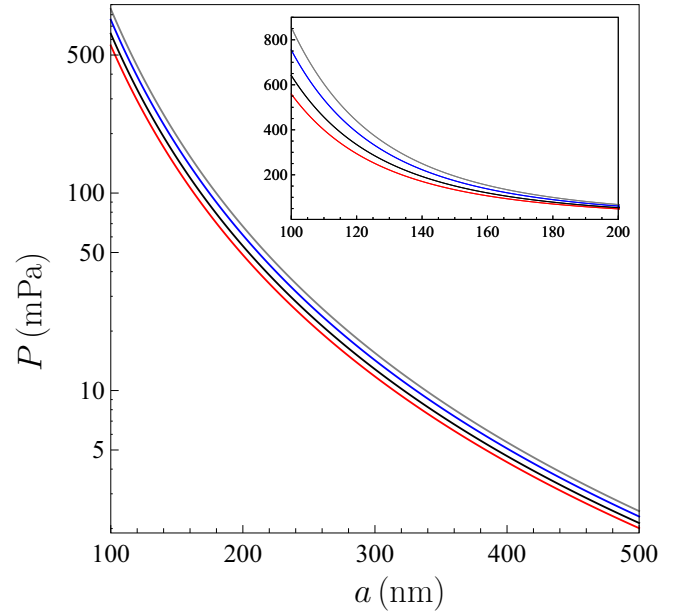

FIG. 1. The Casimir pressure in peptide films containing $\Phi = 0$, 0.1, 0.25, and 0.4 fractions of water deposited on an Au substrate are shown as functions of film thickness in a logarithmic scale by the four lines from bottom to top, respectively, at $T = 300$ K. In the inset, the region of smaller film thicknesses is shown in a uniform scale.

graphene one should put $r_\kappa^{(\text{gr})}(\zeta_l, y) = 0$ in Eq. (11) so that

$$R_\kappa(\zeta_l, y) = r_\kappa^{(1,0)}(\zeta_l, y), \quad (20)$$

where $r_\kappa^{(1,0)}$ is defined in Eq. (6).

To compute the Casimir pressure in peptide film deposited on an Au substrate, one also needs the values of dielectric permittivity of Au, $\varepsilon_l^{(2)}$, at the imaginary Matsubara frequencies. These are usually found by using the optical data for the complex index of refraction of Au [59] extrapolated down to zero frequency and the Kramers-Kronig relations [32]. It has been known that in calculations of the Casimir force between metallic plates through a vacuum gap an extrapolation of the optical data was made by means of either the dissipative Drude model or dissipationless plasma model with diverged results. In so doing, contrary to expectations, theoretical results using the plasma model extrapolation were confirmed experimentally and using the Drude model extrapolation were experimentally excluded [32,60,61] (see also recent Ref. [62]). This is known as the Casimir puzzle [63].

In our case, however, both extrapolations lead to coinciding results because the TE reflection coefficient on the boundary plane between peptide and vacuum vanishes at zero frequency. In the presence of a graphene sheet on top of peptide film both extrapolations lead to almost coinciding results because the TE reflection coefficient on the boundary between graphene and vacuum at zero frequency is very small.

In Fig. 1, we present in the logarithmic scale computational results for the Casimir pressure in peptide films deposited on Au substrate as the functions of film thickness at room temperature $T = 300$ K. The four lines from bottom to top are for the dried films and for films containing $\Phi = 0.1$, 0.25,

and 0.4 volume fractions of water. In the inset, the region of film thicknesses from 100 to 200 nm is shown in a uniform scale. It is seen that in all cases the Casimir pressure remains positive, i.e., the Casimir force is repulsive. Thus, the effects of electromagnetic fluctuations make peptide coating less stable.

As is seen in Fig. 1, the Casimir pressure decreases with increasing film thickness and increases with increasing fraction of water in the film. For instance, for the film of 150 nm thickness containing $\Phi = 0$, 0.1, 0.25, and 0.4 fractions of water the Casimir pressure is equal to 133.8, 150.6, 173.6, and 194.1 mPa, respectively. We have checked that the doping of peptide film with metallic nanoparticles which was used in order to increase film stability in the case of dielectric substrate [49], is incapable of changing the sign of the Casimir pressure for metallic substrates.

Now we consider an effect of graphene coating on top of a dried peptide film. We perform numerical computations of the Casimir pressure using Eqs. (2), (4), (18), and (19) for the cases of pristine graphene which is gapless ($\Delta = 0$) and undoped ($\mu = 0$) and also for graphene characterized either by some nonzero value of Δ (but undoped) or by some nonzero value of μ (but gapless).

In Figs. 2(a) and 2(b) the computational results for the Casimir pressure in graphene-coated dried peptide film are shown as functions of the film thickness by the bottom, middle, and top solid lines for graphene coatings with ($\mu = 0.25$ eV, $\Delta = 0$), ($\mu = \Delta = 0$), and ($\mu = 0$, $\Delta = 0.1$ eV), respectively, at $T = 300$ K in the regions of film thickness (a) from 100 to 180 nm and (b) from 180 to 500 nm. The dashed line reproduces the computational results obtained for a dried peptide film without graphene coating (see the bottom line in Fig. 1). The chosen values of μ and Δ are typical for graphene sheets deposited on a substrate [64].

From Figs. 2(a) and 2(b), it is seen that the presence of a graphene coating strongly affects the Casimir pressure in peptide film. For films of any thickness, this pressure becomes much smaller than in the absence of graphene coating. At some film thickness a_0 the Casimir pressure vanishes and changes its sign from positive to negative for thicker films. This happens at $a_0 = 268.5$ nm for the graphene coating with $\mu = 0$, $\Delta = 0.1$ eV and at $a_0 = 211.7$ nm for a pristine graphene [see the top and middle lines in Fig. 2(b)]. For graphene with $\mu = 0.25$ eV, $\Delta = 0$ [the bottom lines in Figs. 2(a) and 2(b)] we have $a_0 < 100$ nm.

In all cases the presence of graphene coating leads to attractive Casimir forces for sufficiently thick peptide films and, thus, contribute to the film stability. In doing so an increase of μ results in larger magnitudes of the negative Casimir pressures over the wider region of film thicknesses, as compared to the case of pristine graphene, whereas an increase of Δ leads to smaller in magnitude negative pressures than for a pristine graphene and for thicker films. As an example, for a peptide film of 150 nm thickness the Casimir pressure is equal to 133.8 mPa in the absence of a graphene sheet [see Fig. 1 and the dashed line in Fig. 2(a)] but to 24.24, 12.35, and –13.04 mPa in the presence of graphene sheets with ($\mu = 0$, $\Delta = 0.1$ eV), ($\mu = \Delta = 0$), and ($\mu = 0.25$ eV, $\Delta = 0$), respectively [see the top, middle, and bottom solid lines in Fig. 2(a)].
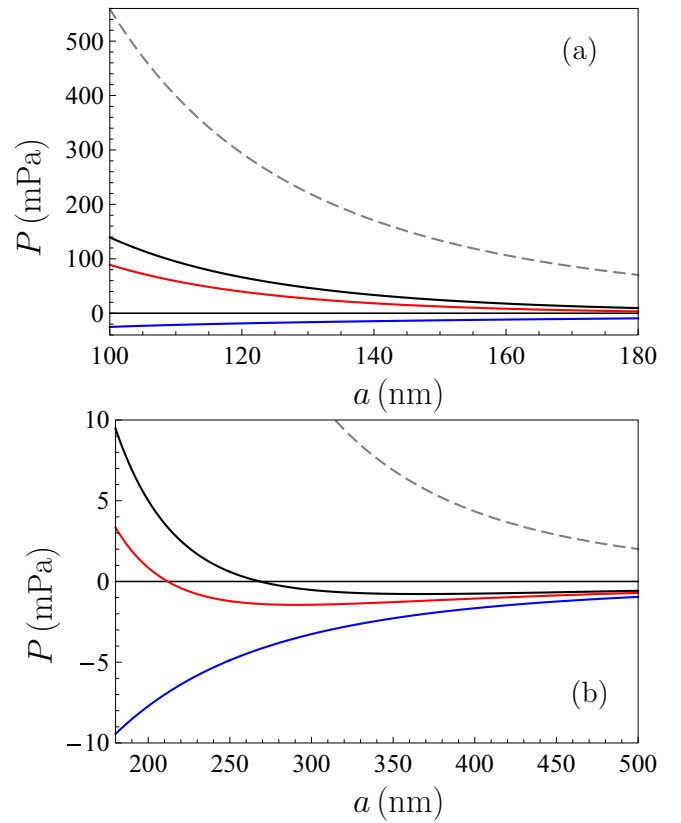

FIG. 2. The Casimir pressure in dried peptide film deposited on an Au substrate and coated by a graphene sheet with ($\mu = 0.25$ eV, $\Delta = 0$), ($\mu = \Delta = 0$), and ($\mu = 0$, $\Delta = 0.1$ eV) are shown as functions of film thickness by the three solid lines from bottom to top, respectively, at $T = 300$ K in the regions of film thickness (a) from 100 to 180 nm and (b) from 180 to 500 nm. The dashed line shows the Casimir pressure in the absence of a graphene layer.

In the end of this section, we compute the value of a_0, where the Casimir pressure in dried peptide film vanishes, as a function of the chemical potential of a graphene sheet for different values of its energy gap. The computational results are shown in Fig. 3 by the four lines from bottom to top for $\Delta = 0$, 0.1, 0.15, and 0.2 eV, respectively. As is seen in Fig. 3, with increasing μ the quantity a_0 decreases. However, an increase of Δ, especially at small μ, results in significant increase of a_0. These results are in agreement with Figs. 2(a) and 2(b) and show that although graphene coating increases the stability of peptide film deposited on a metallic substrate, nonzero values of the chemical potential and the energy gap of graphene influence on this stability in the opposite directions by increasing and decreasing it, respectively.

IV. THE CASE OF DOPED AND GAPPED GRAPHENE COATINGS

In this section, we present the results of numerical computations of the Casimir pressure in a graphene-coated peptide film deposited on an Au substrate in the most realistic case when peptide contains some fraction of water whereas graphene is characterized by nonzero values of both the energy gap and chemical potential.
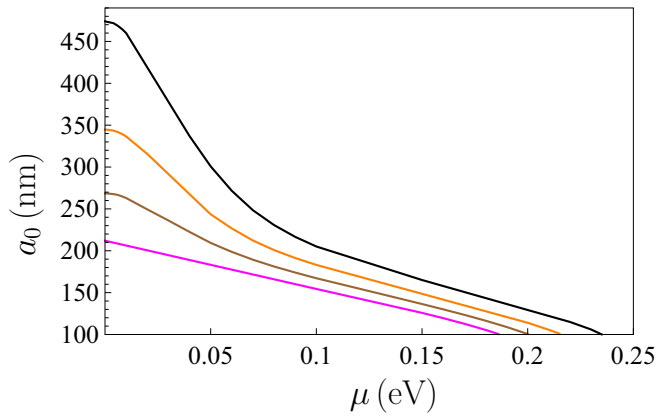
FIG. 3. The thicknesses of dried peptide films deposited on an Au substrate and coated by a graphene sheet such that the Casimir pressure in the film computed at $T = 300$ K vanishes are shown as functions of graphene chemical potential by the four lines from bottom to top for the values of graphene energy gap $\Delta = 0, 0.1, 0.15$, and 0.2 eV, respectively.

Computations are again performed by Eq. (2) where the reflection coefficients are presented in Eqs. (4), (18), and (19). First we consider the peptide film containing $\Phi = 0.1$ fraction of water. The computational results for the Casimir pressure (2) at $T = 300$ K are presented by the pairs of lines labeled 1 and 2 as functions of film thickness in the region (a) from 150 to 250 nm and (b) from 250 to 600 nm. The lines in the pair labeled 1 are computed for graphene sheets with $\mu = 0.02$ eV and the lines in the pair labeled 2 for graphene sheet with $\mu = 0.25$ eV. In each pair, the bottom line is for graphene with $\Delta = 0.1$ eV and the top line is for graphene with $\Delta = 0.2$ eV. Note that graphene coating with relatively low chemical potential $\mu = 0.02$ eV was used in the first experiment on measuring the Casimir interaction in graphene systems [65]. The results of this experiment were found in good agreement with theoretical predictions using the polarization tensor of graphene [50].

Figure 4 allows one to trace the joint impact of nonzero energy gap and chemical potential on the Casimir pressure in peptide film containing 10% of water. The pair of lines labeled 1 is always above the pair labeled 2 because it is computed for smaller chemical potential. Taking into account that in each pair the top line is computed with a larger value of the energy gap, it is again seen that an increase of the chemical potential and the energy gap act on the Casimir pressure in opposite directions. If to compare the pairs of lines labeled 1 and 2, it is seen also that with increasing μ an impact of the energy gap on the Casimir pressure is considerably reducing.

As is seen in Fig. 4(a), the lines of the pair labeled 2 (graphene coating with $\mu = 0.25$ eV) intersect the a axis for the film thicknesses $a_0 = 176.4$ nm (graphene coating with $\Delta = 0.1$ eV) and $a_0 = 190.2$ nm (graphene coating with $\Delta = 0.2$ eV). For thicker peptide films coated with graphene sheets the Casimir pressure becomes negative which corresponds to attraction. For graphene coating with $\mu = 0.02$ eV this happens for larger film thicknesses. From Fig. 4(b) it is seen that the bottom and top lines of the pair labeled 1 (graphene coatings with $\Delta = 0.1$ and 0.2 eV, respectively) intersect the a axis
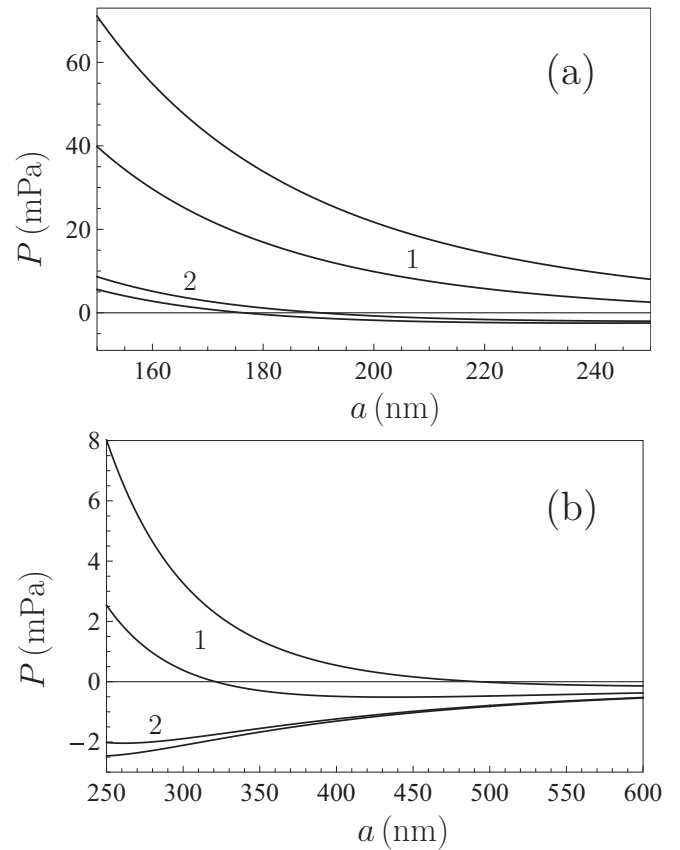

FIG. 4. The Casimir pressures in peptide film containing 10% of water deposited on an Au substrate and coated with a graphene sheet are shown as functions of film thickness by the pairs of lines labeled 1 and 2 for the chemical potential of graphene equal to 0.02 and 0.25 eV, respectively, at $T = 300$ K in the regions of film thickness (a) from 150 to 250 nm and (b) from 250 to 600 nm. In each pair, the bottom and top lines are for graphene with the energy gap equal to 0.1 and 0.2 eV, respectively.

for the film thicknesses $a_0 = 321$ and 493 nm, respectively. Only for thicker films the Casimir pressure becomes attractive in this case.

These results can be compared with those presented in Fig. 3 for a dried peptide film. From Fig. 3 it follows that for $\mu = 0.25$ eV the values of $a_0 < 100$ nm for any $0 \leqslant \Delta \leqslant 0.2$ eV. For $\mu = 0.02$ eV from Fig. 3 it is seen that $a_0 = 249.4$ nm for a graphene sheet with $\Delta = 0.1$ eV and 419.0 nm for a graphene sheet with $\Delta = 0.2$ eV. Thus, in all cases an addition of 10% of water to a peptide film substantially increases the minimum film thickness such that the Casimir pressure in it becomes attractive due to graphene coating.

For comparison purposes, we present the values of the Casimir pressure P (mPa) in peptide film of 150 nm thickness coated by graphene sheets with different values of μ and Δ. The obtained pressures are the following: 39.84 (for $\mu = 0.02$ eV, $\Delta = 0.1$ eV), 71.10 (for $\mu = 0.02$ eV, $\Delta = 0.2$ eV), 5.608 (for $\mu = 0.25$ eV, $\Delta = 0.1$ eV), and 8.657 (for $\mu = 0.25$ eV, $\Delta = 0.2$ eV). It is seen that an increase of Δ with constant μ increases the value of the Casimir pressure whereas an increase of μ with a constant Δ decreases it in agreement with the previously obtained results.
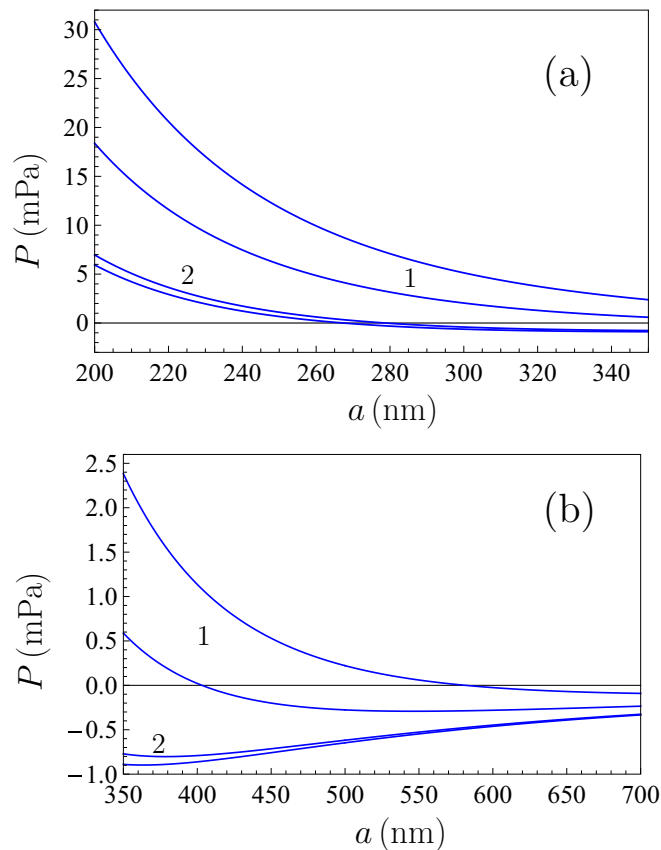
FIG. 5. The Casimir pressures in peptide film containing 25% of water deposited on an Au substrate and coated with a graphene sheet are shown as functions of film thickness by the pairs of lines labeled 1 and 2 for the chemical potential of graphene equal to 0.02 and 0.25 eV, respectively, at $T = 300$ K in the regions of film thickness (a) from 200 to 350 nm and (b) from 350 to 700 nm. In each pair, the bottom and top lines are for graphene with the energy gap equal to 0.1 and 0.2 eV, respectively.
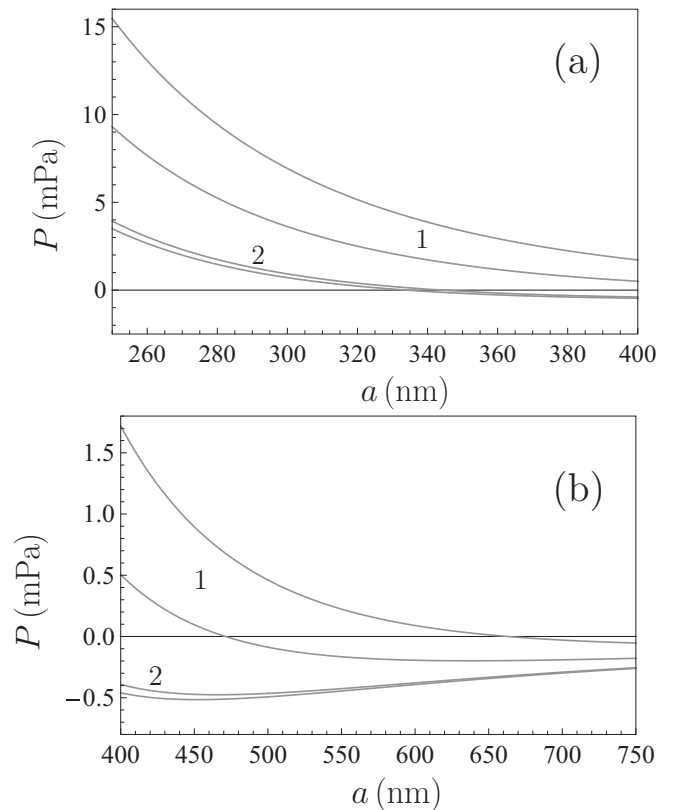

FIG. 6. The Casimir pressures in peptide film containing 40% of water deposited on an Au substrate and coated with a graphene sheet are shown as functions of film thickness by the pairs of lines labeled 1 and 2 for the chemical potential of graphene equal to 0.02 and 0.25 eV, respectively, at $T = 300$ K in the regions of film thickness (a) from 250 to 400 nm and (b) from 400 to 750 nm. In each pair, the bottom and top lines are for graphene with the energy gap equal to 0.1 and 0.2 eV, respectively.

Next we consider the Casimir pressure in peptide film containing $\Phi = 0.25$ fraction of water. Numerical computations were performed in the same way and using the same parameters of a graphene sheet as discussed above in the case $\Phi = 0.1$. The computational results are presented in Figs. 5(a) and 5(b) similarly to Fig. 4. As is seen in Fig. 5(a), for graphene sheets with $\mu = 0.25$ eV, $\Delta = 0.1$ eV and $\mu = 0.25$ eV, $\Delta = 0.2$ eV (bottom and top lines in the pair labeled 2) the Casimir pressure vanishes for the films of thickness $a_0 = 267.5$ and 278.7 nm, respectively.

From Fig. 5(b) we obtain that for graphene sheets with lower doping concentration ($\mu = 0.02$ eV) the Casimir pressure vanishes for the peptide film thicknesses $a_0 = 403.2$ and 581.5 nm for the energy gap of graphene sheet $\Delta = 0.1$ and 0.2 eV, respectively (bottom and top lines in the pair labeled 1). A comparison with the previously obtained results for peptide films containing 10% of water shows that an increase of the percentage of water further increases the values of film thickness delivering zero value of the Casimir pressure by means of a graphene coating.

As expected, an increase of the fraction of water in peptide film of the same thickness results in larger Casimir pres-

sures. Thus, for a film of 150 nm thickness containing 25% of water one obtains $P = 66.39, 98.67, 30.00,$ and 33.02 mPa for graphene coatings with $\mu = 0.02$ eV, $\Delta = 0.1$ eV; $\mu = 0.02$ eV, $\Delta = 0.2$ eV; $\mu = 0.25$ eV, $\Delta = 0.1$ eV; and $\mu = 0.25$ eV, $\Delta = 0.2$ eV, respectively (this value of film thickness is not reflected in Fig. 5 aiming to illustrate the effect of change of sign of the Casimir pressure due to graphene coating).

As the last example, we consider the peptide film containing 40% of water ($\Phi = 0.4$). The computational results for the Casimir pressure are presented in Fig. 6 in the same way as in Figs. 4 and 5. These results confirm that with increasing fraction of water in the film the change of sign in the Casimir pressure takes place for thicker films with the same parameters of graphene coating. Specifically, from Fig. 6(a) one obtains $a_0 = 334.0$ nm for a graphene sheet with $\mu = 0.25$ eV, $\Delta = 0.1$ eV and 344.1 nm for $\mu = 0.25$ eV, $\Delta = 0.2$ eV (the pair of lines labeled 2). Similarly, from Fig. 6(b) one finds $a_0 = 468.0$ nm for $\mu = 0.02$ eV, $\Delta = 0.1$ eV and 662.8 nm for $\mu = 0.02$ eV, $\Delta = 0.2$ eV (the pair of lines labeled 1). For peptide films with $a > a_0$ the Casimir pressure becomes attractive due to the role of graphene coating and, thus, contributes to the film stability.

V. CONCLUSIONS AND DISCUSSION

In the foregoing, we have developed the formalism allowing calculation of the fluctuation-induced Casimir pressure in the graphene-coated peptide films deposited on metallic substrates at any temperature. Within this formalism, metal and peptide are described by the frequency-dependent dielectric permittivities and graphene—by the exact polarization tensor in (2+1)-dimensional space-time found in the framework of the Dirac model. For film thicknesses exceeding 100 nm considered in the paper, the Matsubara frequencies contributing to the Casimir effect described by the Lifshitz theory are well in the application region of the Dirac model. Because of this, the used formalism can be considered as well justified and based on first principles of thermal quantum field theory.

The developed formalism was applied to calculate the Casimir pressure in the graphene-coated dried and containing different fractions of water peptide films deposited on a metallic (Au) substrate. In so doing the cases of a pristine graphene, either doped or gapped graphene (which possesses either nonzero energy gap or nonzero chemical potential), and also both gapped and doped graphene were considered. The system of an uncoated peptide film deposited on a metallic substrate deserves attention because the Casimir pressure in this case turns out to be positive and, thus, corresponds to a repulsion by making film less stable. The coating by a graphene sheet is considered as a means to remedy this defect which may hamper using peptide films of less than a micrometer thickness deposited on metallic substrates in organic electronics.

According to our results, the presence of a graphene layer on top of a peptide film significantly decreases the value of the Casimir pressure in the film. It is shown that for the films of sufficiently large thickness a_0 (which varies from about 100 nm to several hundred nanometers) the Casimir pressure vanishes and for thicker films becomes negative by contributing to their stability. Numerical computations performed for typical fractions of water in peptide films and representative values of the energy gap Δ and chemical potential μ of graphene coatings allowed one to conclude that with increasing μ the value of a_0 decreases whereas increase of Δ and fraction of water in the film leads to larger values of a_0.

These results have a simple physical explanation. The point is that in the configuration of an uncoated peptide film on a metallic substrate all Matsubara terms in the Lishitz formula (2) are positive and, thus, contribute to a repulsion. In the presence of a graphene sheet on top of peptide film, the reflection coefficient $R_{\rm TM}$ defined in Eq. (11) contains the positive term due to the reflection coefficient $r_{\rm TM}^{\rm (gr)}$ on a plane between vacuum and graphene and the negative term due to the reflection coefficient $r_{\rm TM}^{(1,0)}$ on a plane between peptide and vacuum (a contribution of the TE polarization is much smaller than of the TM one). For $l = 0$ the positive term in $R_{\rm TM}$ defined in Eq. (18) is dominant, so that starting from some film thickness, when the zero-frequency Matsubara term gives the major contribution to Eq. (2), the Casimir pressure turns out to be negative, i.e., attractive. An increase of μ and Δ leads to an increase and a decrease of the Matsubara term with $l = 0$, respectively, resulting in respective decrease and increase of a_0. In a similar way, an increase of the fraction of water a peptide film leads to larger $\varepsilon_0^{(1)}$ and, thus, to larger magnitudes of the negative term in $R_{\rm TM}(0, y)$ in Eq. (18). The latter in its turn increases the value of a_0.

Computations performed in Secs. III and IV made it possible to determine the joint action of graphene energy gap and chemical potential, as well as the fraction of water in a peptide film, on the Casimir pressure and reliably predict the combination of these parameters which result in the Casimir attraction favorable for the film stability. Taking into account that for a peptide film of 100 nm thickness containing 10% of water at $T = 300$ K the fluctuation-induced free energy contributes from 5% to 20% of the total cohesive energy of a film [44], one can conclude that the role of fluctuation phenomena in organic electronics is an important problem which deserves further investigation.

[1] *Organic Electronics*, edited by G. Meller and T. Grasser (Springer, Heidelberg, 2010).

[2] J. You, L. Dou, K. Yoshimura, T. Kato, K. Ohya, T. Moriarty, K. Emery, C.-C. Chen, J. Gao, G. Li, and Y. Yangb, A polymer tandem solar cell with 10.6% power conversion efficiency, Nat. Commun. **4**, 1446 (2013).

[3] L. Meng, Y. Zhang, X. Wan, C. Li, X. Zhang, Y. Wang, X. Ke, Z. Xiao, L. Ding, R. Xia, H.-L. Yip, Y. Cao, and Y. Chen, Organic and solution-processed tandem solar cells with 17.3% efficiency, Science **361**, 1094 (2018).

[4] C. D. Dimitrakopoulos and P. R. L. Malenfant, Organic thin film transistors for large area electronics, Adv. Mater. **14**, 99 (2002).

[5] M. E. Gershenson, V. Podzorov, and A. F. Morpurgo, Colloquium: Electronic transport in single-crystal organic transistors, Rev. Mod. Phys. **78**, 973 (2006).

[6] C.-Y. Lee, J.-C. Hwang, Y.-L. Chueh, T.-H. Chang, Y.-Y. Cheng, and P.-C. Lyu, Hydrated bovine serum albumin as the gate dielectric material for organic field-effect transistors, Org. Electr. **14**, 2645 (2013).

[7] M. Ma, X. Xu, L. Shi, and L. Li, Organic field-effect transistors with a low driving voltage using albumin as the dielectric layer, RSC Adv. **4**, 58720 (2014).

[8] H. Uoyama, K. Goushi, K. Shizu, H. Nomura, and C. Adachi, Highly efficient organic light-emitting diodes from delayed fluorescence, Nature (London) **492**, 234 (2012).

[9] Q. Zhang, B. Li, S. Huang, H. Nomura, H. Tanaka, and C. Adachi, Efficient blue organic light-emitting diodes employing thermally activated delayed fluorescence, Nat. Photon. **8**, 326 (2014).

[10] M. Natesan and R. G. Ulrich, Protein microarrays, and biomarkers of infection disease, Int. J. Mol. Sci. **11**, 5165 (2010).

[11] C.-K. Chou, N. Jing, H. Yamaguchi, P.-H. Tsou, H.-H. Lee, C.-T. Chen, Y.-N. Wang, S. Hong, C. Su, J. Kameoka, and M.-C. Hung, Rapid detection of two-protein interaction with a single fluorophore by using a microfluidic device, Analyst **135**, 2907 (2010).

[12] H. Chandra, P. J. Reddy, and S. Srivastava, Protein microarrays and novel detection platforms, Expert Rev. Proteomics **8**, 61 (2011).

[13] B. Zheng, D. T. Haynie, H. Zhong, K. Sabnis, V. Surpuriya, N. Pargaonkar, G. Sharma, and K. Vistakula, Design of peptides for thin films, coatings and microcapsules for applications in biotechnology, J. Biomater. Sci. Polymer Edit. **16**, 285 (2005).

[14] B. Li, D. T. Haynie, N. Palath, and D. Janisch, Nanoscale biomimetics: Fabrication and optimization of stability of peptide-based thin films, J. Nanosci. Nanotechnol. **5**, 2042 (2005).

[15] M. Righi, G. L. Puleo, I. Tonazzini, G. Giudetti, M. Cecchini, and S. Micera, Peptide-based coatings for flexible implantable neural interfaces, Sci. Rep. **8**, 502 (2018).

[16] T. Guterman and E. Gazit, Toward peptide-based bioelectronics: Reductionist design of conductive pili mimetics, Bioelectron. Med. (Lond.) **1**, 131 (2018).

[17] J. Yu, J. R. Horsley, and A. D. Abell, Peptides as bio-inspired electronic materials: An electrochemical and first-principles perspective, Acc. Chem. Res. **51**, 2237 (2018).

[18] S. S. Panda, H. E. Katz, and J. D. Tovar, Solid-state electrical applications of protein and peptide based nanomaterials, Chem. Soc. Rev. **47**, 3640 (2018).

[19] A. Arul, S. Sivagnanam, A. Dey, O. Mukherjee, S. Ghosh, and P. Das, The design and development of short peptide-based novel smart materials to prevent fouling by the formation of non-toxic and biocompatible coatings, RSC Adv. **10**, 13420 (2020).

[20] U. Haas, A. Haase, V. Satzinger, H. Pichler, G. Leising, G. Jakopic, B. Stadlober, R. Houbertz, G. Domann, and A. Schmitt, Hybrid polymers as tunable and directly patternable gate dielectrics in organic thin-film transistors, Phys. Rev. B **73**, 235339 (2006).

[21] L. Romaner, G. Heimel, J.-L. Brédas, A. Gerlach, F. Schreiber, R. L. Johnson, J. Zegenhagen, S. Duhm, N. Koch, and E. Zojer, Impact of Bidirectional Charge Transfer and Molecular Distortions on the Electronic Structure of a Metal-Organic Interface, Phys. Rev. Lett. **99**, 256801 (2007).

[22] H. Yamane, A. Gerlach, S. Duhm, Y. Tanaka, T. Hosokai, Y. Y. Mi, J. Zegenhagen, N. Koch, K. Seki, and F. Schreiber, Site-Specific Geometric and Electronic Relaxations at Organic-Metal Interfaces, Phys. Rev. Lett. **105**, 046103 (2010).

[23] M. G. Helander, M. T. Greiner, Z. B. Wang, and Z. H. Lu, Effect of electrostatic screening on apparent shifts in photoemission spectra near metal/organic interfaces, Phys. Rev. B **81**, 153308 (2010).

[24] A. V. Nenashev, S. D. Baranovskii, M. Wiemer, F. Jansson, R. Österbacka, A. V. Dvurechenskii, and F. Gebhard, Theory of exciton dissociation at the interface between a conjugated polymer and an electron acceptor, Phys. Rev. B **84**, 035210 (2011).

[25] S. Ciuchi and S. Fratini, Electronic transport and quantum localization effects in organic semiconductors, Phys. Rev. B **86**, 245201 (2012).

[26] S. Pittner, D. Lehmann, D. R. T. Zahn, and V. Wagner, Charge transport analysis of poly(3-hexylthiophene) by electroreflectance spectroscopy, Phys. Rev. B **87**, 115211 (2013).

[27] S. Ono and K. Ohno, Minimal model for charge transfer excitons at the dielectric interface, Phys. Rev. B **93**, 121301(R) (2016).

[28] Y. Zhang, J. Qiao, S. Gao, F. Hu, D. He, B. Wu, Z. Yang, B. Xu, Y. Li, Y. Shi, W. Ji, P. Wang, X. Wang, M. Xiao, H. Xu, J.-B. Xu, and X. Wang, Probing Carrier Transport and Structure-Property Relationship of Highly Ordered Organic Semiconductors at the Two-Dimensional Limit, Phys. Rev. Lett. **116**, 016602 (2016).

[29] K. Stallberg, A. Namgalies, and U. Höfer, Photoluminescence study of the exciton dynamics at PTCDA/noble-metal interfaces, Phys. Rev. B **99**, 125410 (2019).

[30] C. Metzger, M. Graus, M. Grimm, G. Zamborlini, V. Feyer, M. Schwendt, D. Lüftner, P. Puschnig, A. Schöll, and F. Reinert, Plane-wave final state for photoemission from nonplanar molecules at a metal-organic interface, Phys. Rev. B **101**, 165421 (2020).

[31] V. A. Parsegian, *Van der Waals Forces: A Handbook for Biologists, Chemists, Engineers, and Physicists* (Cambridge University Press, Cambridge, 2005).

[32] M. Bordag, G. L. Klimchitskaya, U. Mohideen, and V. M. Mostepanenko, *Advances in the Casimir Effect* (Oxford University Press, Oxford, 2015).

[33] E. M. Lifshitz and L. P. Pitaevskii, *Statistical Physics*, Pt. II (Pergamon Press, Oxford, 1980).

[34] V. A. Parsegian and B. W. Ninham, Application of the Lifshitz theory to the calculation of van der Waals forces across thin lipid films, Nature (London) **224**, 1197 (1972).

[35] S. Nir, Van der Waals interactions between surfaces of biological interest, Progr. Surf. Sci. **8**, 1 (1976).

[36] C. M. Roth, B. L. Neal, and A. M. Lenhoff, Van der Waals interactions involving proteins, Biophys. J. **70**, 977 (1996).

[37] B.-S. Lu and R. Podgornik, Effective interactions between fluid membranes, Phys. Rev. E **92**, 022112 (2015).

[38] G. L. Klimchitskaya and V. M. Mostepanenko, Casimir free energy of metallic films: Discriminating between Drude and plasma model approaches, Phys. Rev. A **92**, 042109 (2015).

[39] G. L. Klimchitskaya and V. M. Mostepanenko, Casimir and van der Waals energy of anisotropic atomically thin metallic films, Phys. Rev. B **92**, 205410 (2015).

[40] G. L. Klimchitskaya and V. M. Mostepanenko, Casimir free energy and pressure for magnetic metal films, Phys. Rev. B **94**, 045404 (2016).

[41] G. L. Klimchitskaya and V. M. Mostepanenko, Characteristic properties of the Casimir free energy for metal films deposited on metallic plates, Phys. Rev. A **93**, 042508 (2016).

[42] G. L. Klimchitskaya and V. M. Mostepanenko, Low-temperature behavior of the Casimir free energy and entropy of metallic films, Phys. Rev. A **95**, 012130 (2017).

[43] G. L. Klimchitskaya and V. M. Mostepanenko, Casimir free energy of dielectric films: Classical limit, low-temperature behavior and control, J. Phys.: Condens. Matter **29**, 275701 (2017).

[44] M. A. Baranov, G. L. Klimchitskaya, V. M. Mostepanenko, and E. N. Velichko, Fluctuation-induced free energy of thin peptide films, Phys. Rev. E **99**, 022410 (2019).

[45] G. Löffler, H. Schreiber, and O. Steinhauser, Calculation of the dielectric properties of a protein and its solvent: Theory and a case study, J. Mol. Biol. **270**, 520 (1997).

[46] P. Adhikari, A. M. Wen, R. H. French, V. A. Parsegian, N. F. Steinmetz, R. Podgornik, and W.-Y. Ching, Electronic structure, dielectric response, and surface charge distribution of RGD (1FUV) peptide, Sci. Rep. **4**, 5605 (2014).

[47] E. N. Velichko, M. A. Baranov, and V. M. Mostepanenko, Change of sign in the Casimir interaction of peptide films deposited on a dielectric substrate, Mod. Phys. Lett. A **35**, 2040020 (2020).

[48] V. M. Mostepanenko, E. N. Velichko, and M. A. Baranov, Role of electromagnetic fluctuations in organic electronics, J. Electr. Sci. Tech. **18**, 100023 (2020).

[49] G. L. Klimchitskaya, V. M. Mostepanenko, and E. N. Velichko, Effect of increased stability of peptide-based coatings in the Casimir regime via nanoparticle doping, Phys. Rev. B **102**, 161405(R) (2020).

[50] G. L. Klimchitskaya, U. Mohideen, and V. M. Mostepanenko, Theory of the Casimir interaction for graphene-coated substrates using the polarization tensor and comparison with experiment, Phys. Rev. B **89**, 115419 (2014).

[51] A. H. Castro Neto, F. Guinea, N. M. R. Peres, K. S. Novoselov, and A. K. Geim, The electronic properties of graphene, Rev. Mod. Phys. **81**, 109 (2009).

[52] M. Bordag, I. V. Fialkovsky, D. M. Gitman, and D. V. Vassilevich, Casimir interaction between a perfect conductor and graphene described by the Dirac model, Phys. Rev. B **80**, 245406 (2009).

[53] I. V. Fialkovsky, V. N. Marachevsky, and D. V. Vassilevich, Finite-temperature Casimir effect for graphene, Phys. Rev. B **84**, 035446 (2011).

[54] G. Bimonte, G. L. Klimchitskaya, and V. M. Mostepanenko, Thermal effect in the Casimir force for graphene and graphene-coated substrates: Impact of nonzero mass gap and chemical potential, Phys. Rev. B **96**, 115430 (2017).

[55] C. Henkel, G. L. Klimchitskaya, and V. M. Mostepanenko, Influence of chemical potential on the Casimir-Polder interaction between an atom and gapped graphene or graphene-coated substrate, Phys. Rev. A **97**, 032504 (2018).

[56] M. Bordag, G. L. Klimchitskaya, V. M. Mostepanenko, and V. M. Petrov, Quantum field theoretical description for the reflectivity of graphene, Phys. Rev. D **91**, 045037 (2015); **93**, 089907(E) (2016).

[57] M. Bordag, I. Fialkovskiy, and D. Vassilevich, Enhanced Casimir effect for doped graphene, Phys. Rev. B **93**, 075414 (2016); **95**, 119905(E) (2017).

[58] G. L. Klimchitskaya and V. M. Mostepanenko, Origin of large thermal effect in the Casimir interaction between two graphene sheets, Phys. Rev. B **91**, 174501 (2015).

[59] *Handbook of Optical Constants of Solids*, edited by E. D. Palik (Academic Press, New York, 1985).

[60] G. L. Klimchitskaya, U. Mohideen, and V. M. Mostepanenko, The Casimir force between real materials: Experiment and theory, Rev. Mod. Phys. **81**, 1827 (2009).

[61] L. M. Woods, D. A. R. Dalvit, A. Tkatchenko, P. Rodriguez-Lopez, A. W. Rodriguez, and R. Podgornik, Materials perspective on Casimir and van der Waals interactions, Rev. Mod. Phys. **88**, 045003 (2016).

[62] G. Bimonte, B. Spreng, P. A. Maia Neto, G.-L. Ingold, G. L. Klimchitskaya, V. M. Mostepanenko, and R. S. Decca, Measurement of the Casimir Force between 0.2 and $8\,\mu$m: Experimental procedures and comparison with theory, Universe **7**, 93 (2021).

[63] V. M. Mostepanenko, Casimir puzzle and Casimir conundrum: Discovery and search for resolution, Universe **7**, 84 (2021).

[64] P. Shemella and S. K. Nayak, Electronic structure and band-gap modulation of graphene via substrate surface chemistry, Appl. Phys. Lett. **94**, 032101 (2009).

[65] A. A. Banishev, H. Wen, J. Xu, R. K. Kawakami, G. L. Klimchitskaya, V. M. Mostepanenko, and U. Mohideen, Measuring the Casimir force gradient from graphene on a SiO_2 substrate, Phys. Rev. B **87**, 205433 (2013).